

Cyclopalladated Complexes of 3-Thiophosphorylbenzoic Acid Thioamides: Hybrid Pincer Ligands of a New Type. Synthesis, Catalytic Activity, and Photophysical Properties

V. A. Kozlov,[†] D. V. Aleksanyan,[†] Yu. V. Nelyubina,[†] K. A. Lyssenko,[†] E. I. Gutsul,[†]
L. N. Puntus,[‡] A. A. Vasil'ev,[§] P. V. Petrovskii,[†] and I. L. Odinets^{*,†}

A. N. Nesmeyanov Institute of Organoelement Compounds, Russian Academy of Sciences, 28 Vavilova Street, Moscow 119991, Russian Federation, Institute of Radioengineering and Electronics, Russian Academy of Sciences, 11-7 Mokhovaya Street, Moscow 125009, Russian Federation, and N. D. Zelinsky Institute of Organic Chemistry, Russian Academy of Sciences, 47 Leninsky Prospekt, 117913 Moscow, Russian Federation

Received March 28, 2008

Treatment of the 3-diphenylphosphorylbenzoic acid amides **3a,b** with the Lawesson reagent resulted in 3-diphenylthiophosphorylbenzoic acid thioamides **4a,b**, which easily underwent cyclopalladation at the C-2 position of the central benzene ring to give new hybrid pincer complexes **5a,b** with κ^3 -SCS coordination. Molecular structures of the complexes were characterized by X-ray diffraction. The peculiarities of chemical bonding in **5a** were investigated via topological analysis of charge density in the crystal. The palladium complexes **5a,b** demonstrated high catalytic activity for the Suzuki cross-coupling reactions of aryl bromides with phenylboronic acid and exhibited luminescence at 77 and 300 K.

Introduction

Despite pincer-type complexes having been known for more than 30 years, they are still the subject of unflagging interest due to high catalytic activity in different processes such as dehydrogenation of alkanes, reduction of ketones, aldol condensation, and cross-coupling reactions.^{1–3} These complexes allow one to finely tune the reactivity of the metal center by adjusting the steric and electronic properties of donor atoms. Over the years the classic pincer-type ligand of B. Shaw^{4–6} containing a phenyl backbone and methylene bridges between donor atoms (as a rule P, N, S, and O atoms) has been modified and developed. In particular, isophthalic acid thioamides containing two thiocarbonyl groups as coordination sites undergo metalation to afford two five-membered metallacycles with a σ -C(phenyl)–metal bond (where the metal is platinum or palladium) and may be regarded as nonclassic SCS-pincer type ligands.^{7–13} Not so long ago T. Kanbara and T. Yamamoto described the synthesis and

molecular structures of Pd and Pt complexes of 1,3-(bisthiophosphoryl)benzene.¹⁴ The platinum complexes formed by SCS-pincer ligands of both types and palladium complexes of dithioamide pincer ligands possess luminescent properties in the solid state, broadening the scope of useful luminophores for optical and electroluminescence devices.

Taking these results into account, it seems interesting to develop the synthetic approach to a hybrid ligand of the SCS-pincer type bearing one thiophosphoryl and one thiocarbonyl group as potential coordinating sites and investigate its ability to undergo cyclometalation. Therefore, in this communication we report the synthesis of such ligands and their palladium complexes, which proved to be active catalysts for the Suzuki reaction and exhibit moderate luminescence in the solid state at 77 and 300 K.

Results and Discussion

Synthesis and Catalytic Activity of Complexes. A convenient synthetic route for the synthesis of the desired thioamide-thiophosphoryl-based SCS-pincer ligands has been elaborated starting from easily available 3-diphenylphosphorylbenzoic acid, **1** (Scheme 1). In turn, the acid **1** was obtained by reaction of the Grignard reactant 1-bromo-3-methylbenzene with diphenylchlorophosphine oxide followed by oxidation using KMnO₄ according to the procedure described in the literature.¹⁵ Transformation of phosphorylated acid **1** to the corresponding acid chloride and aminolysis performed as a one-pot process resulted in amides **2a,b** in good yields. It should be noted that the

* Corresponding author. E-mail: odinets@ineos.ac.ru.

[†] A. N. Nesmeyanov Institute of Organoelement Compounds.

[‡] Institute of Radioengineering and Electronics.

[§] N. D. Zelinsky Institute of Organic Chemistry.

(1) Albrecht, M.; van Koten, G. *Angew. Chem., Int. Ed.* **2001**, *40*, 3750.

(2) van der Boom, M. E.; Milstein, D. *Chem. Rev.* **2003**, *103*, 1759.

(3) Singleton, J. T. *Tetrahedron.* **2003**, *59*, 1837.

(4) Shaw, B. L.; Moulton, C. J. *J. Chem. Soc., Dalton Trans.* **1976**, 1020.

(5) Shaw, B. L.; Crocker, C.; Errington, R. J.; McDonald, W. S.; Odell, K. J.; Goodfellow, R. J. *J. Chem. Soc., Chem. Commun.* **1979**, 498.

(6) Shaw, B. L.; Errington, J.; McDonald, W. S. *J. Chem. Soc., Dalton Trans.* **1980**, 2312.

(7) Takahashi, S.; Nonoyama, M.; Kita, M. *Trans. Met. Chem.* **1995**, *20*, 528.

(8) Nojima, Y.; Nonoyama, M. *Polyhedron.* **1996**, *15*, 3795.

(9) Hossain, M. A.; Lucarimi, S.; Powell, D.; Bowman-James, K. *Inorg. Chem.* **2004**, *43*, 7275.

(10) Kanbara, T.; Okada, K.; Yamamoto, T.; Ogawa, H.; Inoue, T. *J. Organomet. Chem.* **2004**, *689*, 1860.

(11) Akaiwa, M.; Kanbara, T.; Fukumoto, H.; Yamamoto, T. *J. Organomet. Chem.* **2005**, *690*, 4192.

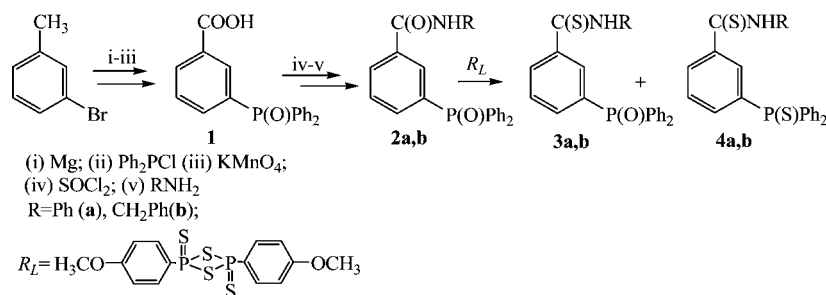
(12) Okamoto, K.; Kanbara, T.; Yamamoto, T. *Chem. Lett.* **2006**, *35*, 558.

(13) Begum, R. A.; Powell, D.; Bowman James, K. *Inorg. Chem.* **2006**, *45*, 964.

(14) Kanbara, T.; Yamamoto, T. *J. Organomet. Chem.* **2003**, *688*, 15.

(15) Chvetz, A. A.; Sukhorukov, Yu. I.; Bulgarevich, S. B.; Zvetkov, E. N. *Russ. J. Gen. Chem.* **1978**, *48*, 1986.

Scheme 1. Synthesis of Thioamide-Thiophosphoryl-Based S,C,S-Pincer Ligands



corresponding amide was used in excess, as 3-diphenylphosphorylbenzoic acid chloride was formed as the corresponding

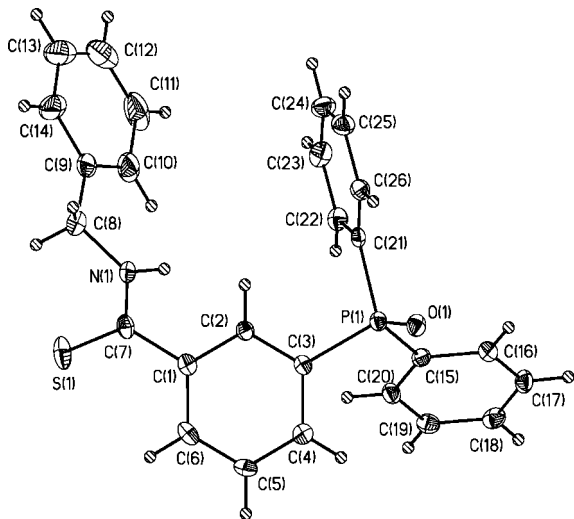


Figure 1. General view of the molecule of thioamide **3b** with representation of atoms by thermal ellipsoids ($p = 50\%$).

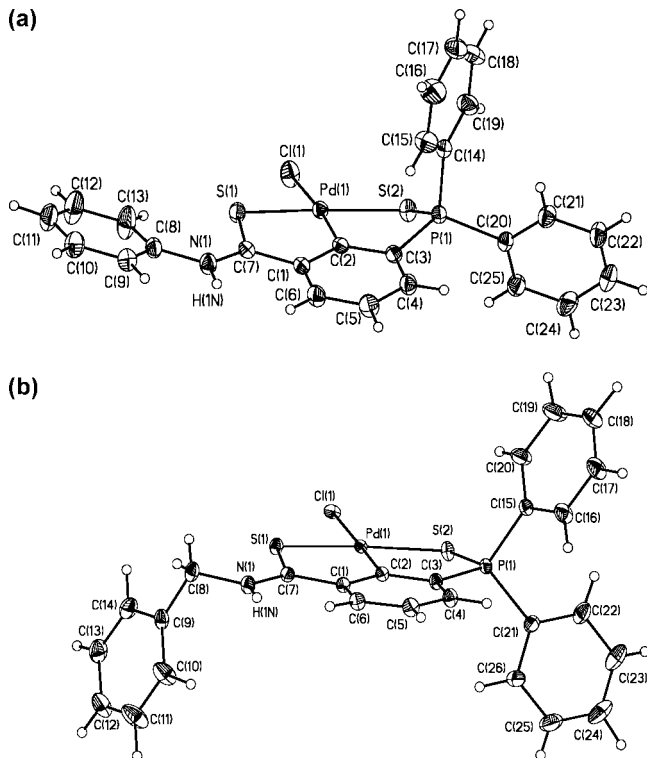


Figure 2. General view of **5a(B)** and **5b** with the representation of atoms by thermal ellipsoids ($p = 50\%$) and numbering scheme.

hydrochloride. Further thionation of the oxygen precursors **2a,b** with the Lawesson reagent under refluxing in xylene proceeded as a step-by-step process and provided a mixture of the corresponding thioamides **3a,b** and **4a,b** bearing diphenylphosphoryl and diphenylthiophosphoryl groups, respectively. With the other conditions being equal (reaction time 15 h) the ratio of S,O:S,S products in the crude reaction mixtures estimated by ³¹P NMR techniques depended on the substituents at the amide group and changed from 1:1.5 in the case of **3a:4a** to 1.5:1 for **3b:4b**. This reduction of the S,S-thioamide **4b** yield may be connected with the decreased thermal stability of aralkylthioamide **4b** in comparison with thioanilide **4a**. Fortunately, the corresponding couples of thioamides (**3a** and **4a**, **3b** and **4b**) can be easily separated by column chromatography.

Structures of the compounds **2–4** bearing O,O-, S,O-, and S,S-functionalities were unambiguously confirmed by NMR, IR, and elemental analysis data. In the ³¹P NMR spectra the signals were observed in the regions typical for phosphine oxides for compounds **2a,b** and **3a,b** (ca. 28–29 ppm) or for phosphine sulfides (47.18 and 42.48 ppm for **4a** and **4b**, respectively). In spite of the presence of a great number of phenyl substituents in the molecules, the ¹H and ¹³C NMR spectra of the compounds can be interpreted rather easily, as signals of a central phenyl core differ from those belonging to phenyl groups at both the phosphorus and nitrogen atoms. Thus, in the ¹H NMR spectra of amides **2–4** the doublet signal of the hydrogen atom at the 2-position of the central benzene core had the most downfield shift (8.10–8.50 ppm), with the coupling constant ³J_{PH} ranging from 12.0 to 13.7 Hz. In a similar manner, the signals of the central benzene ring observed in the ¹³C NMR spectra along with the downfield-shifted signal of the thiocarbonyl carbon atom and phenyl moieties of (thio)phosphoryl and amido groups can be assigned unambiguously. IR spectra of 3-diphenyl(thio)phosphorylbenzoic acid amides and thioamides **2–4** demonstrated absorption bands typical for functionalities such as C=O, P=O, and P=S, present in the particular compound.

The molecular structure of intermediate phosphorylated thioamide **3b** was confirmed by X-ray analysis (Figure 1). In the crystal both thioamide and phosphoryl groups do not participate in conjugation with the center aromatic ring and significantly deviate from its plane with the corresponding torsion angles O(1)P(1)C(3)C(2) and S(1)C(7)C(1)C(2) equal to 107.8° and 137.5°, respectively. Although this conformation can be the consequence of steric repulsion, we also cannot exclude the role of crystal-packing effects, namely, the formation of an intermolecular N–H···O=P hydrogen bond (O···N 2.785(2) Å).

The reaction of **4a,b** with PdCl₂(PhCN)₂ in CH₂Cl₂ readily proceeded as cyclopalladation of the central phenyl ring to form the corresponding SCS-pincer palladium complexes **5a,b** (Scheme 2). It should be noted that related O,S-thioamides **3a,b** did not react with PdCl₂(PhCN)₂, suggesting that double S,S-coordina-

Scheme 2. Synthesis of Palladacycles

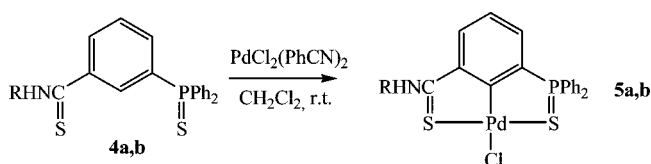


Table 1. Palladacycle-Catalyzed Suzuki Cross-Coupling

catalyst	mol %	X	yield (%)
5a	3	-C(O)CH ₃	94
	3	-C(O)CH ₃	100
5b	3 ^a	-C(O)CH ₃	100
	1		100
	0.3		100
	0.3 ^a	-C(O)CH ₃	99
	0.1	-C(O)CH ₃	100
	0.1 ^a		97
5b	3	-CH ₃	97
5b	1	-CH ₃	86
5a	3	-OCH ₃	80
5b	3	-OCH ₃	84

^a Without Bu₄NBr.

tion was a crucial factor for cyclopalladation. Complexes **5a,b** spontaneously crystallized from the reaction mixture as bright yellow high-melting solids, poorly soluble in most organic solvents. They are stable to air and moisture and are thermally stable up to >285 °C.

The structure of the κ^3 -SCS complexes **5a,b** was assigned on the basis of downfield chemical shifts (ca. 58 ppm) in the ³¹P NMR spectra, indicating the coordination of the palladium atom with the sulfur atom of the phosphine sulfide group, the absence of the signals for the C2-hydrogen atoms, being situated between two substituents in the ¹H NMR spectra, and a strong downfield shift up to ca. 169 ppm of the signals belonging to the C2 carbon atom in the ¹³C NMR spectra. The last two facts are strong evidence of Pd–C bond formation. The presence in the ¹H NMR spectra of the signals of the hydrogen atoms of a thioamide group being downfield shifted compared with those in the free ligands indicated the formation of a Pd–S(C) coordination bond. In general, the ¹³C NMR spectra for **5a,b** are consistent with the literature data for symmetric Pd(II) SCS-pincer complexes.^{10,11,14}

Taking into account that the palladium-catalyzed Suzuki reaction is one of the most effective methods for the construction of C_{aryl}–C_{aryl} bonds, we tested complexes **5a,b** for cross-coupling of *para*-substituted bromobenzenes and phenylboronic acid. Even the preliminary results of the ongoing studies showed a high conversion value in the case of activated bromobenzenes (Table 1). The normal dependence¹⁶ on the electron-withdrawing properties of the substituent X at the aryl bromide was observed in both cases, although complex **5b**, bearing a benzyl substituent at the nitrogen atom, was a little more active. Using this compound as a representative example, it was demonstrated that the quantitative conversion was observed even when 0.1 mol % of the catalyst was used. The monitoring of the reaction mixtures by ³¹P spectra revealed that complexes **5a,b** remained unchanged after the cross-coupling reaction, excluding the possible changing of the Cl anion for the bromine one in the presence of Bu₄NBr as a component of the reaction mixture.

However, such anion exchange does not influence the chemical shift of the complexes in the ³¹P NMR spectra. The stability of the complexes explains the high activity of the catalyst used in smaller amounts. It is interesting to note that in the absence of ammonium salt the conversion was the same as when 0.3–3 mol % of the catalyst was used and slightly decreased when the latter was used in smaller amount.

Comparing the catalytic activity of the new complexes with reported results for the palladium pincer complexes with SCS-coordination we may mention that complexes formed by 1,3-bis[(*tert*-butylthio)methyl]benzene have been found to catalyze the Suzuki cross-coupling of *p*-bromotoluene and benzeneboronic acid.¹⁶ At the typical catalyst loading (1 mol %) a 69% yield of phenyltoluene has been achieved. As for palladium SCS-pincer complexes of the same kind as **5a,b**, i.e., bearing thioamide or phosphine sulfide moieties as coordination sites, complexes of isophthalic acid were tested in the Heck reaction only,¹³ while the data concerning the catalytic activity of those formed by 1,3-bis(thiophosphoryl)benzene are absent in the literature.

Regardless of the fact that both complexes did not show activity in the reaction with 2-chloroacetophenone, where precipitation of palladium black indicated that ArCl did not form the product of oxidation addition to such palladacycles, the search of the active catalysts among those comprising hybrid SCS-ligands of similar structure seems rather promising.

Molecular Geometry and Crystal Structure of Palladium Complexes 5a,b. Crystals of **5a** and **5b** (Figures 2 and 3) suitable for X-ray analysis were obtained by slow crystallization from CH₂Cl₂ solutions. It should be mentioned that application of different solvents for recrystallization resulted in the formation of two different crystals of **5a**. Thus, the crystal solid obtained via slow crystallization from CH₂Cl₂ resulted in the crystalline solvate with two independent molecules of **5a(A)** via 1.5 CH₂Cl₂. Additional washing of this crystalline solid by Et₂O resulted in a crystals lacking the DCM solvate molecule and having only one independent molecule of **5a(B)**.

In general, the geometry of the square-planar Pd moiety in **5a** and **5b** (Table 1) is similar to that for the pincer Pd complexes formed by isophthalic acid thioamides¹¹ and 3,5-bis(diphenylthiophosphoryl)benzene¹⁴ excluding slight asymmetry, i.e., the difference of Pd–S bonds for C=S and P=S groups.

It was reasonable to propose that factors such as the nature of the substituent at the N(1) atom, conjugation of the phenyl ring with the thioamide group, and conformation of the metallocycle would lead to some variations of molecular geometry and in particular for the C(2)Pd(1)S(1)S(2)Cl(1) fragment. At first glance, the pronounced difference of three independent molecules of **5a** in two crystals, **5a(A)** and **5a(B)**, should lead at least to some variation of bond lengths for the thioamide fragment. Indeed, the increase of the dihedral angle between the phenyl ring and the thioamide group in **5a(A)** (62.9–69.7°) with respect to **5a(B)** (12°) causes a shortening of the N(1)–C(8) bond in the latter due to conjugation with the phenyl moiety (Table 2). Despite this variation, N(1)–C(7) bond lengths in all independent molecules of both **5a** and **5b** are nearly the same. As a consequence, C(1)–C(7), C(7)–S(1), and Pd(1)–S(1) bond lengths are almost equal for all complexes studied. It should be noted that the C(7)–S(1) bond in **5a** and **5b** is significantly shortened in comparison to **3b** (1.495(3) Å), thus indicating that in pincer complexes a thioamide group is involved in conjugation with the central aromatic ring. In turn, the P(1)–C(3) bond lengths are almost independent of the

Table 2. Principle Geometrical Parameters of **5a** and **5b**

	5a(A) I	5a(A) II	5a(B)	5b
Bond Lengths				
Pd(1)–C(2)	1.981(4)	1.971(4)	1.972(2)	1.9720(6)
Pd(1)–S(1)	2.277(1)	2.263(1)	2.2640(6)	2.2775(2)
Pd(1)–S(2)	2.341(1)	2.325(1)	2.3436(6)	2.3202(2)
Pd(1)–Cl(1)	2.399(9)	2.401(1)	2.4066(7)	2.3980(2)
S(1)–C(7)	1.695(4)	1.697(4)	1.698(2)	1.7068(7)
S(2)–P(1)	2.004(1)	2.010(1)	2.0018(9)	2.0137(3)
P(1)–C(3)	1.793(4)	1.787(4)	1.791(2)	1.7873(8)
N(1)–C(7)	1.314(5)	1.329(4)	1.325(3)	1.316(1)
C(1)–C(7)	1.464(5)	1.460(5)	1.470(3)	1.470(1)
N(1)–C(8)	1.440(6)	1.444(4)	1.428(3)	1.465(3)
Conformation of Five-Membered Metalacycles ^a				
5CS	env. (C(1) 0.10 Å)	env. (S(1) 0.19 Å)	env. (Pd(1) 0.22 Å)	env. (S(1) 0.27 Å)
5PS	env. (P(1) 0.25 Å)	env. (S(2) 0.28 Å)	tw. (P(1)/S(2) –0.43/0.33 Å)	env. (S(2) 0.27 Å)

^a For a description of conformation, its type (envelope (env.) or twist (tw.)), the particular atom deviating from the plane of the rest of the atoms, and values of the deviation are given.

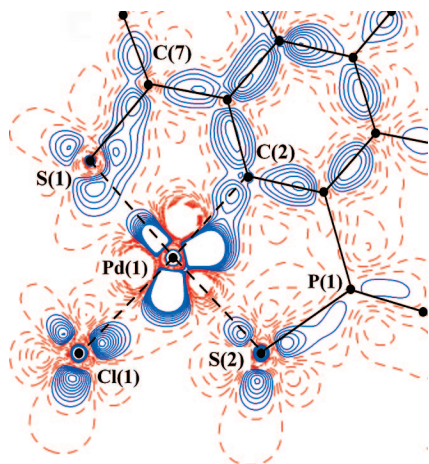


Figure 3. Section of the static deformation electron density in the plane of atoms C(2), S(1), and Cl(1) in **5b**. Contours are drawn with $0.1 \text{ e } \text{Å}^{-3}$ steps; the nonpositive contours are dashed.

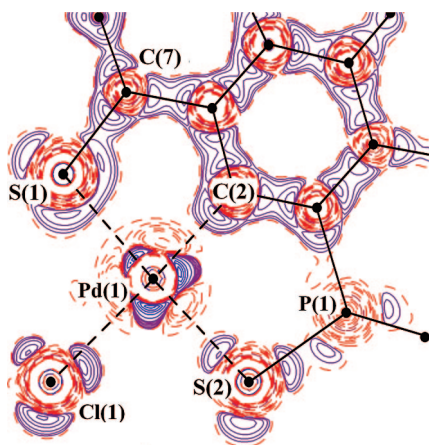


Figure 4. Experimental $-\nabla^2\rho(r)$ distribution in the area of the Pd(1)–S interactions in **5b**. The contours are drawn through $10 \text{ e } \text{Å}^{-5}$, and the nonpositive contours are dashed.

conformation of the P=X moiety and are nearly the same in **5a**, **5b** and **3b** ($1.806(2) \text{ Å}$).

Furthermore, the geometry of the palladium complexes **5** does not depend on the conformations of the five-membered metallacycles containing P=S (5PS) and C=S bonds (5CS), which are different (Table 2). Mostly, the conformation of the five-membered cycles presents an envelope, while the twist conformation is found for 5PS in **5a(B)**. In addition to the type of

conformation, the puckering degree and the specific atom deviating from the plane of the rest of the atoms of the cycles are also different.

The difference in conformations leads in turn to the variation of mutual disposition of the phenyl ring π -system and the palladium d-orbitals. Indeed, using the bent angle (φ), i.e., the dihedral angles between planes Pd(1)C(7)P(1)Cl(1) and C(7)P(1)–C(1)C(2)C(3)C(4)C(5)C(6), as a parameter, we can conclude that in the case of **5b** and one independent molecule of **5a(A)** the aromatic ring C(1)–C(6) is coplanar (φ is 1.1° and 3.3° , respectively) with the PdS₂CCl ring. In contrast, in the second independent molecule of **5a(A)** and in **5a(B)** φ is as much as 9.8° and 15.5° , respectively.

Clearly such variation of conformation and φ is solely the consequence of crystal-packing effects. In all complexes the N–H group participates in the formation of N–H \cdots Cl intermolecular H-bonds, assembling the molecules into infinite chains. Excluding **5a(B)**, N–H \cdots Cl hydrogen bonds are characterized by similar proton donor to acceptor distances (N(1) \cdots Cl(1)) equal to $3.154(3)$ – $3.179(3) \text{ Å}$, while in **5a(B)** the corresponding distance increases to $3.484(4) \text{ Å}$. In addition to the above H-bond in all structures there is a number of weak C–H \cdots S and C–H \cdots Cl interactions that can also be responsible for variation of the molecular conformation.

Despite all of the above differences in the molecular geometry the Pd–C, Pd–S, and Pd–Cl distances for **5a** and **5b** are almost identical, thus indicating that the molecular geometry is rather stable and cannot be used for estimation of chemical bonding peculiarities. At the same time such variations can be sufficient to significantly affect the luminescent properties of the complexes (see below).

The crystalline complexes **5a** and **5b** can be considered as ideal systems for the examination of the nature and energy aspects of σ -C(phenyl)–Pd and Pd–S bonding in SCS-pincer complexes. Therefore, we performed a detailed analysis of the electron density distribution in the crystal of **5b**, within Bader's "atoms in molecules" (AIM) theory,¹⁷ on the basis of the high-resolution XRD data for this particular compound.

The AIM theory has been applied both experimentally and theoretically to a wide variety of structures containing many

(17) (a) Bader, R. F. W. *Atoms in Molecules. A Quantum Theory*; Clarendon Press: Oxford, 1990. (b) Bader, R. F. W. *J. Chem. Phys. A* **1998**, *102*, 7314.

Table 3. Topological Parameters for the Pd–X (X = C, S, Cl) Bonds in the Crystal of 5b

	$\rho(\mathbf{r})$, e \AA^{-3}	$\nabla^2\rho(\mathbf{r})$, e \AA^{-5}	$h_e(\mathbf{r})$, au	$g(\mathbf{r})$, au	$-\nu(\mathbf{r})$, au	E_{cont} , kcal/mol
Pd(1)–C(2)	0.989	6.45	–0.094659	0.161519	0.256178	80.4
Pd(1)–S(1)	0.580	7.51	–0.036665	0.114566	0.151231	47.5
Pd(1)–S(2)	0.529	5.24	–0.023061	0.077373	0.100434	31.5
Pd(1)–Cl(1)	0.442	6.72	–0.007349	0.077045	0.084395	26.5

different types of intermolecular interactions.¹⁸ The energy of the bonding interactions is estimated using the correlation found between the energy of the contact (E_{cont}) and the value of the potential energy density function $\nu(\mathbf{r})$ in the corresponding bond critical point (3, –1).¹⁹

It should be noted that although the number of investigation of charge density for heavy atoms²⁰ significantly increased over the last years, topological analysis of electron density in the crystal of 4d metals is still rather rare.²¹ Moreover, to the best of our knowledge for the pincer complex of 3d and 4d metals both theoretical and experimental analyses were not yet performed.

According to the static deformation electron density (DED) map in the section of the Pd(1) moiety (Figure 3) in **5b**, the DED distribution is characterized by the expected features, thus, to some extent, indicating the correctness of analytical electron density function obtained. In particular, accumulation of DED is observed in the areas of covalent bonds of the ligand. At the same time, there is the depletion of the density between the interacting atoms for the Pd–X (X = Cl, S, C) bonds, demonstrating the substantial “closed-shell” character. The peaks of DED function attributed to electron lone pairs (LPs) are located in the vicinity of the chlorine, sulfur, and carbon C(1) atoms. The $-\nabla^2\rho(\mathbf{r})$ distribution (Figure 4) also exhibits the same features. The latter is consistent with the ellipticity (ϵ), which serves as a measure of bond deviation from the cylindrical symmetry (see ref 17), for P–S and C–S bonds (ϵ is 0.36 and 0.19) indicating their double-bond character. The higher value in the case of the former agrees well with the increase of ellipticity, as one passes from 2 to 3 period elements. Both $\rho(\mathbf{r})$ and $-\nabla^2\rho(\mathbf{r})$ distributions in the section under consideration are also characterized by the significant anisotropy around Pd(1), presumably resulting from the splitting of 4d-orbitals of the palladium atom under a distorted square-planar environment. The occupancies of the latter were estimated by means of the technique proposed by Holladay et al.²² Before the calculation, x and y axes were directed to the corners of the S₂Pd(C)Cl square and the z axis was directed to its normal. According to this analysis, the d_{z^2} (2.04 e), d_{xz} (1.99 e), and d_{yz} (1.92 e) orbitals of the Pd²⁺ ion are most populated, while the occupancy of $d_{xy}/d_{x^2-y^2}$ is 1.84/1.34 e, respectively. The value of the total d-population was found to be very close to the expected one and equal to 7.91 e.

The interactions of the palladium with the pincer ligand can be considered as partly being of “peak-to-hole” type. Thus, the LPs of coordinating S(2) and C(1) atoms are directed toward the areas of the electron density depletion near the Pd(1) one. However, in the case of Pd–Cl and Pd–S(1) interactions the regions of DED accumulation of the palladium and chlorine/sulfur species are located in a “peak-to-peak” fashion. The charge distribution for the C(phenyl)–Pd bond agrees with the assumption that the lone pair at carbon participates in the σ -bonding via overlap with a d-orbital of appropriate symmetry at the palladium atom. At the same time, in the interatomic area instead of the DED accumulation the depletion of the latter is observed, which is common for the interactions between atoms with closed shells. Thus, the C(phenyl)–Pd bond also displays a significant component of electrostatic character along with that in the S₂PdCl moiety. Furthermore, although Pd–S bond lengths are quite similar, on the basis of the difference in the electron density arrangement for the corresponding regions one can expect their strength to be rather different. However, since it is difficult to draw any conclusion on the matter from the directionality for these two interactions, the estimation of their energies on the quantitative level is an interesting challenge.

For this purpose we have performed a search for bond critical points (3, –1) (hereinafter BCPs) of the $\rho(\mathbf{r})$ function in the area of the palladium fragment in **5b**. They were located for all of the above bonds. On the basis of the topological parameters (see Table 3) in the corresponding BCPs, the Pd–X (X = Cl, S, C) interactions are of intermediate type, with the positive $\nabla^2\rho(\mathbf{r})$ and negative electron energy $h_e(\mathbf{r})$ values being in the range of 5.24–7.51 e \AA^{-5} and –0.094659 to –0.007349 au, respectively. The ratio of potential/kinetic energy densities ($\nu(\mathbf{r})/g(\mathbf{r})$) indicates the lowering degree of shared character in the series of X = C(2), S(1), S(2), and Cl(1) atoms. Accordingly, one can expect the strength of the bonds under consideration to vary in a similar fashion. Their energies (E_{cont}) were estimated via the correlation between the latter and the $\nu(\mathbf{r})$ value in the BCP for the corresponding interaction. Thus, the E_{cont} (Table 3) values were found to be in good agreement with the above assumption; that is, the σ -C(phenyl)–Pd bond is the strongest one, while the energy of the Pd–Cl interaction amounts only to 26.5 kcal/mol. Apparently, such high energy of the palladium–carbon σ -bond (80.4 kcal/mol) is responsible for the greater stability of Pd(II) pincer complexes as compared with traditional catalysts as well as the far smaller contamination of the Pd-catalyzed reaction product with palladium residues. In analogy, the energy of the metal–carbon bond in the case of similar Pt(II)-based complexes possessing the same features under a wide variety of reaction conditions will be of the same order of magnitude or even larger.

In crystalline **5b** the smallest of the E_{cont} values for the Pd–S bonds is attributed to the interaction with the shorter interatomic distance, namely, Pd(1)–S(1). This correlates well with the predominant “electrostatic” component of the contacts formed by the palladium cation and sulfur atoms of the pincer ligand. Moreover, although the difference in the corresponding bond lengths is hardly meaningful, the $E_{\text{Pd(1)–S(1)}} - E_{\text{Pd(1)–S(2)}}$ value exceeds 15 kcal/mol, which falls, for instance, in the energy

(18) (a) Koritsanszky, T. S.; Coppens, P. *Chem. Rev.* **2001**, *101*, 1583. (b) Gatti, C. Z. *Kristallogr.* **2005**, *220*, 399. (c) Tsirelson, V. G.; Ozerov, R. P. *Electron Density and Bonding in Crystals: Principles, Theory and X-Ray Diffraction Experiments in Solid State Physics and Chemistry*; IOP Publishing Ltd., 1996.

(19) (a) Espinosa, E.; Molins, E.; Lecomte, C. *Chem. Phys. Lett.* **1998**, *285*, 170. (b) Espinosa, E.; Alkorta, I.; Rozas, I.; Elguero, J.; Molins, E. *Chem. Phys. Lett.* **2001**, *336*, 457.

(20) Coppens, P.; Iversen, B.; Larsen, F. K. *Coord. Chem. Rev.* **2005**, *249*, 179.

(21) (a) Pillet, S.; Guang, Wu.; Kulsomphob, V. Benjamin, Harvey, G.; Ernst, R. D.; Coppens, P. *J. Am. Chem. Soc.*, **2003**, *125*, 1937. (b) Borissova, A. O.; Antipin, M. Yu.; Perekalin, D. S.; Lyssenko, K. A. *CrystEngComm* **2008**, DOI: 10.1039/b716776h.

(22) Holladay, A.; Leung, P. C.; Coppens, P. *Acta Crystallogr.* **1983**, *A39*, 377.

range common for hydrogen bonds of intermediate strength. Hence, care must be taken in the application of the geometrical approach for defining the nonequivalency of the Pd–S bonds in the case of κ^3 -SCS-pincer complexes.

Obviously, the distribution of Pd–S bonds as observed in crystalline **5b** is very likely to affect the integral characteristics of the sulfur atoms. The charges for the central palladium moiety were obtained by the integration of the $\rho(\mathbf{r})$ function over atomic basins (Ω) surrounded by a zero-flux surface. Thus, the values of the atomic charges are equal to 0.65/–0.50 e for palladium/chlorine and –0.81/–0.45 e in the case of S(2)/S(1). Significant electron density remains on the carbon C(1) (its charge is 0.26 e). The same parameter for P(1) and C(7) atoms was found to be 1.02 and 0.43 e, respectively. In line with the charges, the volumes of sulfur atoms, evaluated in the similar fashion, also demonstrate a certain discrepancy (31.97 and 30.55 Å³). However, this trend can be partly caused by the participation of S(1) and S(2) atoms in the formation of different numbers of intermolecular interactions.

As mentioned above, in the solid state **5b** (as well as related **5a**) molecules are self-assembled into infinite chains by intermolecular N–H \cdots Cl contacts with the N \cdots Cl separation being 3.1762(5) Å (the corresponding value in the case of **5a** is equal to 3.1534(10) Å). These associates are held together through weaker interactions of C–H groups with chlorine/sulfur atoms, a π -system of phenyl rings, and weak π – π stacking interactions between the phenyl ring connected with the phosphorus atom and the central aromatic ring. It is important to indicate that on the basis of the geometrical criteria one can distinguish two C–H \cdots S contacts for S(2) and only one in the case of S(1). The search for BCPs in their area revealed that the corresponding number for the atom S(2) amounts to 4, while for the second one it is equal to 3. In both cases the intermolecular interactions are of “closed-shell” type and characterized by very small values of E_{cont} (as compared with the above coordination bonds), being in the range 0.3–2.4 kcal/mol. The total energy of the contacts formed by atoms S(1) and S(2) is only 3.8 and 2.7 kcal/mol, respectively. Thus, one can consider the influence of the above contacts on the atomic parameters of both sulfur atoms to be infinitesimal. For comparison, the N–H \cdots Cl hydrogen bond contributes 3.8 kcal/mol.

Photophysical Properties. The absorption spectra of **4a,b** in CH₂Cl₂ at 293 K (Figure S1) display a very intense broad band situated higher than 250 nm, assigned to a transition mainly involving orbitals located on the thiosphoryl groups, and less intense bands at 31 250 cm^{–1} (320 nm, $\epsilon = 7000 \text{ M}^{-1} \text{ cm}^{-1}$) and 33 990 cm^{–1} (295 nm, $\epsilon = 4200 \text{ M}^{-1} \text{ cm}^{-1}$), respectively, corresponding to transitions mainly located on the aromatic rings. The weakest bands observed at 23 530 cm^{–1} (425 nm, $\epsilon = 360 \text{ M}^{-1} \text{ cm}^{-1}$) and 25 565 cm^{–1} (390 nm, $\epsilon = 140 \text{ M}^{-1} \text{ cm}^{-1}$) in the solutions of **4a** and **4b**, respectively, are attributed to n– π^* transitions²³ (Table 4). The absorption spectra for the complexes **5a,b** (Figure S2) contain also overlapped bands in the region 330–450 nm, which can be caused by the participation of the Pd center in these electronic transitions. These bands are similar to those of the reported pincer palladium complexes, in which the corresponding absorption bands have been tentatively assigned to a spin-allowed 4d(Pd) $\rightarrow \pi^*(\text{L})$ (metal-to-ligand charge transfer, MLCT) transition.^{11,14,23} The absorption band of **5a** (440 nm) attributed to a MLCT state has a bathochromic shift upon comparison with that of **5b** (430 nm),

suggesting a reduction in the energy level of the π^* -orbital of the ligand upon the transition from the Ph substituent at the nitrogen atom to PhCH₂.

The ligands **4a,b** are not light-emitting at room and low temperatures, whereas moderate luminescence was observed for all complexes as a microcrystalline sample at 77 K as well as in frozen DMF solution (Figures 5 and 6). The bands observed in the luminescence spectra of frozen solutions were assigned to MLCT states according to other pincer palladium complexes.^{11,14} The small difference in λ_{em} for the frozen solutions of **5a** and **5b** can be explained by the effect of phenyl and benzyl moieties, which is quite reasonable, but the opposite sign of their difference in comparison with absorption data (see Table 4) is probably determined by the stabilization of some particular conformations in frozen solutions at 77 K in comparison with their superposition at room temperature.

The emissions with maxima at ~ 660 and 710 nm were observed at 77 K for microcrystalline samples of **5a(A)** and **5a(B)**, **5b**, respectively. Since the Pd–Pd distance between adjacent complexes is 7.983, 7.032, and 7.941 Å, respectively, and an extended π -stacking interaction is absent, the excimer contribution to the emission observed is unlikely. We tentatively concluded that the emission occurs from the MLCT excited states, similar to the published palladium and platinum complexes.^{10,11,14} Interestingly, the same λ_{em} is observed for **5a(B)** and **5b**, while these complexes contain different substituents on the pincer ligand. Since the latter leads to the different positions of the MLCT state in solutions, it is logical to suggest that the structural features of complex and its packing can influence the positions of the MLCT state and as a consequence the λ_{em} of the microcrystalline samples. It is worth mentioning that the same crystals were used for luminescence measurements and for X-ray experiments, and the position of the emission line is independent of the excitation wavelength. On the one hand, φ (dihedral angle between plane of the phenyl ring π -system and palladium d-orbitals) equals 1.1° and the aromatic ring C(1)–C(6) is coplanar with PdS₂CCl in **5b**, while φ is 15.5° in **5a(B)**. On the other hand, the dihedral angle between the phenyl ring and the thioamide group in **5a(B)** is only 12°, which causes a shortening of the N(1)–C(8) bond described above, while in **5b** the ligand contains a PhCH₂ substituent situated below the PdS₂C plane and forms an angle of around 70°. Hence the similar energy of the MLCT states observed for microcrystalline samples of **5a(B)** and **5b** is probably the result of the combined influence of conjugation of phenyl with the thioamide group and the conformation of the metallacycle.

Weak luminescence was detected for complex **5a(B)** at room temperature also with λ_{em} equal to 740 nm (see Figure S3). Room-temperature luminescence of mononuclear Pd(II) complexes is very rare, usually because of the presence of low-lying metal-centered (MC) excited states, which deactivate the potentially luminescent metal-to-ligand charge transfer (MLCT) and ligand-centered (LC) levels through thermally activated surface-crossing processes.²⁴ Therefore the lack of the room-temperature luminescence for **5a(A)** and **5b** is not unexpected, and probably the luminescence observed for **5a(B)** originates from the more optimal position of the MLCT state concerning the position of the MC states.

Conclusion

To summarize the results presented, we developed a synthetic route to novel SCS-pincer ligands, namely, 3-diphenylthiophos-

(23) Lai, S.-W.; Cheung, T. C.; Chan, N. C. W.; Cheung, K. K.; Peng, S.-M.; Che, C.-M. *Inorg. Chem.* **2000**, *39*, 255.

(24) Neve, F.; Crispini, A.; Pietro, C. D.; Campagna, S. *Organometallics* **2002**, *21*, 3511.

Table 4. Photophysical Data for 4a, 4b, 5a, and 5b

compound	λ_{max}^a (ϵ) [nm ($\text{M}^{-1} \text{cm}^{-1}$)]	λ_{em}^b /nm	λ_{em}^c /nm
4a	320 (7000), 425 (360)		
4b	295 (4200), 390 (140)		
5a	330 (3410), 375 (3450), 440 ^d (920)	620	660/710 ^e
5b	335 (5610), 365 (5930), 430 ^d (1340)	640	710

^a Absorption maxima in CH_2Cl_2 at room temperature. ^b Emission maximum in frozen DMF solution at 77 K. ^c Emission maximum of a microcrystalline sample at 77 K. ^d Shoulder peak. ^e Data for **5(A)**/**5a(B)** complexes.

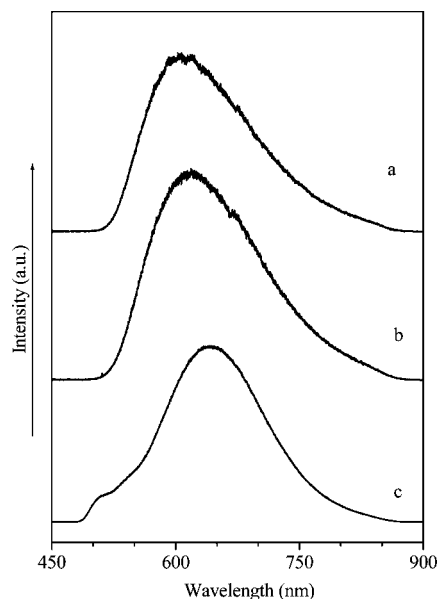


Figure 5. Luminescence spectra of frozen solutions of **5a(A)** (a), **5a(B)** (b), and **5b** (c) in DMF at 77 K.

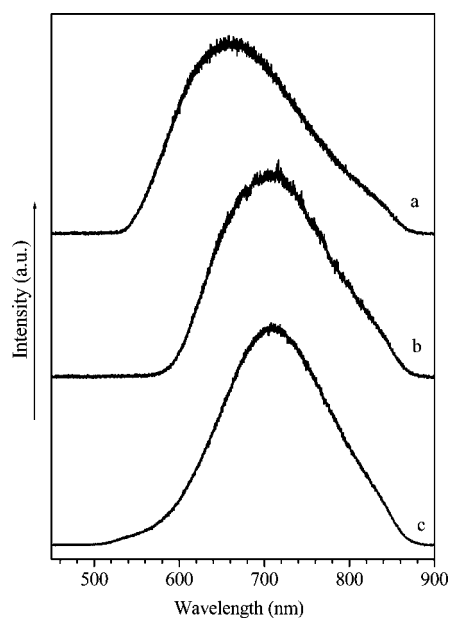


Figure 6. Luminescence spectra of microcrystalline samples of **5a(A)** (a), **5a(B)** (b), and **5b** (c) at 77 K. The emission lifetime amounts to 9.5, 11.0, and 10.8 μs for **5a(A)**, **5a(B)**, and **5b**, respectively.

phorylbenzoic acid thioamides, which easily underwent cyclopalladation at the C-2 position of the central benzene ring to give new hybrid pincer complexes with κ^3 -SCS coordination. The structures of the complexes obtained were investigated in detail in terms of electronic density distribution in the crystal

and the luminescent properties as a function of molecular geometry. The palladium complexes possess photoluminescence even at room temperature and demonstrated high catalytic activity in Suzuki cross-coupling reactions.

Experimental Section

General Remarks. If not noted otherwise all manipulations were carried out without taking precautions to exclude air and moisture. All solvents and chemicals were used as received without further purification if not mentioned. NMR spectra were recorded on Bruker Avance-300 and Bruker Avance-400 spectrometers, and chemical shifts (δ) were internally referenced by the residual solvent signals relative to tetramethylsilane (^1H and ^{13}C) or externally to H_3PO_4 (^{31}P). The ^{13}C NMR spectra were registered using the *JMODECHO* mode; the signals for the C atom bearing odd and even numbers of protons have opposite polarities. IR spectra were recorded in a thin layer on a Fourier "Magna-IR750" (Nicolet) spectrometer, resolution 2 cm^{-1} , 128 scans. The assignment of the absorption bands in the IR spectra was made according to ref 25. Flash chromatography was carried out using Merck silica gel 60 (230–400 mesh ASTM). Melting points were determined with an Electrothermal IA9100 digital melting point apparatus and are uncorrected. The luminescence spectra of compounds investigated were measured with an Avesta ASP-150TF spectrometer.

3-Diphenylphosphoryl-N-phenylbenzamide, 2a. A mixture of 3-diphenylphosphorylbenzoic acid (3.5 g, 10.9 mmol), thionyl chloride (7.5 mL, 109 mmol), and C_6H_6 (30 mL) was refluxed for 3 h. The solvent and the excess SOCl_2 were removed under vacuum to afford 5.5 g of yellow liquid residue (a mixture of 3-diphenylphosphorylbenzoyl chloride and HCl). This residue was diluted by CH_2Cl_2 (25 mL), and then a solution of aniline (1.0 g, 10.9 mmol) in CH_2Cl_2 (5 mL) and pyridine (10 mL) were successively added. The resulting mixture was stirred for 48 h and washed with diluted hydrochloric acid (10 mL concentrated HCl /200 mL of water) and water (150 mL). The organic phase was dried over anhydrous Na_2SO_4 and evaporated to dryness. The resulting residue was crystallized from EtOH to give **1a** (3.5 g, 81.0%) as a white solid. Mp: 243–245 $^\circ\text{C}$ (EtOH). $^{31}\text{P}\{^1\text{H}\}$ NMR (121.49 MHz, $\text{CDCl}_3/\text{DMSO}-d_6$): δ 27.89 ppm. ^1H NMR (400.13 MHz, $\text{CDCl}_3/\text{DMSO}-d_6$): δ 7.02 (t, 1H, H_{Ar}), 7.23 (t, 2H, H_{Ar}), 7.40–7.70 (m, 14H, H_{Ar}), 8.12 (d, 1H, $^3J_{\text{HH}} = 7.5 \text{ Hz}$), 8.28 (d, 1H, $^3J_{\text{PH}} = 12.1 \text{ Hz}$), 9.97 (s, 1H, NH). IR (KBr, ν/cm^{-1}): 542, 694, 725, 763, 1122, 1132, 1181 (P=O), 1326, 1439, 1546 (C(O)NH), 1601 (Ph), 1670 (C=O), 3068, 3137, 3200, 3264, 3294. Anal. Calcd for $\text{C}_{25}\text{H}_{20}\text{NO}_2\text{P}$: C, 75.56; H, 5.07; N, 3.52. Found: C, 75.69; H, 4.94; N, 3.41.

3-Diphenylphosphoryl-N-phenylmethylbenzamide, 2b. A mixture of 3-diphenylphosphorylbenzoic acid (3.8 g, 12 mmol), thionyl chloride (8.9 mL, 120 mmol), and C_6H_6 (30 mL) was refluxed for 3 h. The solvent and the excess SOCl_2 were removed in vacuo. The residue (5.3 g) was diluted in CH_2Cl_2 (25 mL), and this solution was added dropwise to a solution of benzylamine (5.5 g, 51.4 mmol) in CH_2Cl_2 (15 mL) at 10 $^\circ\text{C}$. The reaction mixture was stirred for 6 h and filtered. The filtrate was washed with water (80 mL), dried over anhydrous Na_2SO_4 , evaporated under reduced pressure, washed with ether, and recrystallized from EtOH to yield **2b** (4.7 g, 97%) as a white solid. Mp: 172–174 $^\circ\text{C}$. $^{31}\text{P}\{^1\text{H}\}$ NMR (121.49 MHz, CDCl_3): δ 28.90. ^1H NMR (400.13 MHz, CDCl_3): δ 4.55–4.57 (m, 2H, CH_2), 7.08 (br s, 1H, NH), 7.23–7.27 (m, 6H, H_{Ar}), 7.41–7.63 (m, 11H, H_{Ar}), 8.08 (dd, 1H, $^4J_{\text{HH}} = 0.9 \text{ Hz}$, $^3J_{\text{HH}} = 7.8 \text{ Hz}$), 8.27 (dd, 1H, $^4J_{\text{HH}} = 2.8 \text{ Hz}$, $^3J_{\text{PH}} = 12.0 \text{ Hz}$). IR (KBr, ν/cm^{-1}): 546, 693, 725, 1106, 1119, 1155, 1172 (P=O), 1292,

Table 5. Details of Data Collection and Conventional Refinement of 2c, 5a(A), 5a(B), and 5b

	3b	5a(A)	5a(B)	5b
empirical formula	C ₂₆ H ₂₂ NOPS	C _{51.5} H ₄₁ Cl ₅ N ₂ P ₂ Pd ₂ S ₄	C ₂₅ H ₁₉ CINPPdS ₂	C ₂₆ H ₂₁ CINPPdS ₂
fw	427.48	1268.10	570.35	584.38
T, K	120	100	296	100
space group	<i>P</i> 2 ₁ / <i>c</i>	<i>P</i> $\bar{1}$	<i>P</i> 2 ₁ / <i>c</i>	<i>P</i> 2 ₁ 2 ₁
<i>a</i> , Å	12.2827(9)	11.9887(5)	13.0603(6)	12.7414(6)
<i>b</i> , Å	17.2457(13)	14.6611(6)	13.7939(7)	12.7768(7)
<i>c</i> , Å	10.7969(8)	14.8385(6)	13.2593(7)	15.1936(8)
α , deg		89.829(5)		
β , deg	103.48(2)	84.196(5)	109.845(5)	
γ , deg		87.873(5)		
<i>V</i> , Å ³	2224.0(3)	2592.97(18)	2246.8(2)	2473.4(2)
<i>Z</i>	4	1	4	4
density, g cm ⁻³	1.277	1.624	1.686	1.569
<i>F</i> (000)	896	1270	1144	1176
μ (Mo K α), cm ⁻¹	2.35	12.12	12.16	11.07
diffractometer	Bruker SMART 1000	Bruker SMART APEX2	Bruker SMART APEX2	Bruker SMART APEX2
absorp corr (Mo K α)	semiempirical from equivalents	semiempirical from equivalents	semiempirical from equivalents	semiempirical from equivalents
scan technique	ω -scan	ω -scan	ω -scan	ω -scan
θ_{\max} , deg	29	27	29	55
no. of measd reflns	20 134	21 315	17 888	311 646
no. of indep reflns (<i>R</i> (int))	5858 (0.0604)	11 229 (0.0431)	5955 (0.0260)	31 692 (0.0346)
no. of obsd reflns with <i>I</i> > 2 σ (<i>I</i>)	3671	8171	4743	29 503
wR2	0.1124	0.0667	0.0689	0.0527
R1 (all reflns)	0.0898	0.0660	0.0422	0.0281
R1 (reflns with <i>I</i> > σ (<i>I</i>))	0.0582	0.0384	0.0282	0.0219
GOF	1.001	0.998	1.004	1.005
ρ_{\max}/ρ_{\min} , e Å ⁻³	0.448/-0.369	0.969/-0.615	0.621/-0.343	1.944/-0.729

1436, 1545 (br, C(O)NH), 1650 (C=O), 3030, 3052, 3258. Anal. Calcd for C₂₆H₂₂N₂O₂P: C, 75.90; H, 5.39; N, 3.40. Found: C, 75.47; H, 5.35; N, 3.31.

3-Diphenylphosphoryl-*N*-phenylbenzenecarbothioamide, 3a, and 3-Diphenylthiophosphoryl-*N*-phenylbenzenecarbothioamide, 4a. A mixture of *N*-phenylbenzamide **2a** (2.2 g, 5.5 mmol) and Lawesson reagent (4.5 g, 11 mmol) was refluxed in xylene (50 mL) for 15 h. After cooling to room temperature the mixture was washed with a saturated aqueous solution of Na₂CO₃ and water and dried over Na₂SO₄ followed by purification by silica gel column chromatography (eluent CHCl₃) to give **3a** and **4a**, respectively.

3a: light yellow solid (0.5 g, 22%). Mp: 214–215 °C (EtOAc). ³¹P{¹H} NMR (121.49 MHz, CDCl₃): δ 29.52 ppm. ¹H NMR (400.13 MHz, CDCl₃): δ 7.27–7.61 (m, 15H, H_{Ar}), 7.72 (d, 2H, H_{Ar}, *J* = 7.8 Hz), 8.36 (d, 1H, H_{Ar}, ³*J*_{HH} = 7.1 Hz), 8.50 (d, 1H, H_{Ar}, ³*J*_{PH} = 12.5), 11.16 (br s, 1H, NH). IR (KBr, ν /cm⁻¹): 691, 727, 745, 1114, 1121, 1181 (P=O), 1369, 1412, 1435, 1497, 1551 (C(S)NH), 1598, 2955, 3000, 3050, 3177. Anal. Calcd for C₂₅H₂₀NOPS: C, 72.62; H, 4.88; N, 3.39. Found: C, 72.48; H, 4.85; N, 3.34.

4a: yellow solid (1.0 g, 42%). Mp: 126–128 °C. ³¹P{¹H} NMR (121.49 MHz, DMSO-*d*₆): δ 47.18 ppm. ¹H NMR (400.13 MHz, DMSO-*d*₆): δ 7.28 (t, 1H, H_{Ar}), 7.44 (t, 2H, H_{Ar}), 7.55–7.78 (m, 14H, H_{Ar}), 7.97 (d, 1H, H_{Ar}, ³*J*_{HH} = 7.3 Hz), 8.19 (d, 1H, H_{Ar}, ³*J*_{PH} = 13.7 Hz), 11.92 (s, 1H, NH). ¹³C{¹H} NMR (100.61 MHz, DMSO-*d*₆): δ 124.12 (*o*-C_{Ar}-N), 126.53 (*p*-C_{Ar}-N), 128.62 (C₄, ²*J*_{CP} = 11.7 Hz), 128.63 (*m*-C_{Ar}-N), 128.95 (*m*-C_{Ph}-P, ³*J*_{CP} = 12.1 Hz), 129.94 (C₆, ⁴*J*_{CP} = 2.2 Hz), 131.39 (C₅, ³*J*_{CP} = 12.1 Hz), 131.81 (*o*-C_{Ph}-P, ²*J*_{CP} = 10.6 Hz), 132.03 (*i*-C_{Ph}-P, ¹*J*_{CP} = 85.1 Hz), 132.09 (*p*-C_{Ph}-P), 132.59 (C₃, ¹*J*_{CP} = 84.4 Hz), 133.60 (C₂, ²*J*_{CP} = 10.3 Hz), 139.83 (*i*-C_{Ar}-N), 143.00 (C₁, ³*J*_{CP} = 12.1 Hz), 196.34 (C=S). IR (KBr, ν /cm⁻¹): 510, 638 (P=S), 694, 703, 715, 1101, 1107, 1401, 1435, 1508 (C(S)NH), 1596, 2943, 2972, 3047, 3163. Anal. Calcd for C₂₅H₂₀NPS₂: C, 69.90; H, 4.69; N, 3.26. Found: C, 69.94; H, 4.63; N, 3.10.

3-Diphenylphosphoryl-*N*-phenylmethylbenzenecarbothioamide, 3b. Yield: 62%, yellow solid. Mp: 182–184 °C (C₆H₆). ³¹P{¹H} NMR (121.49 MHz, CDCl₃): δ 29.11 ppm. ¹H NMR (400.13 MHz, CDCl₃): δ 5.01 (d, 2H, CH₂, ³*J*_{HH} = 5.3 Hz),

7.32–7.39 (m, 17H, H_{Ar}), 8.16–8.23 (m, 2H, H_{Ar}), 8.96 (br s, 1H, NH). IR (KBr, ν /cm⁻¹): 527, 539, 552, 693, 698, 724, 750, 960, 1121, 1170 (P=O), 1405, 1437, 1535 (br, (C(S)NH), 2915, 3027, 3178. Anal. Calcd for C₂₆H₂₂NOPS: C, 73.05; H, 5.19; N, 3.28. Found: C, 73.09; H, 5.21; N, 3.14.

3-Diphenylthiophosphoryl-*N*-phenylmethylbenzenecarbothioamide, 4b. Yield: 30%, yellow solid. Mp: 60–63 °C (Et₂O–hexane). ³¹P{¹H} NMR (121.49 MHz, CDCl₃): δ 42.48 ppm. ¹H NMR (400.13 MHz, CDCl₃): δ 4.94 (d, 2H, CH₂, ³*J*_{HH} = 5.7 Hz), 7.26–7.34 (m, 5H, H_{Ar}), 7.56–7.72 (m, 12H, H_{Ar}), 7.91–7.94 (m, 1H, H_{Ar}), 8.09–8.13 (m, 1H, H_{Ar}), 10.93 (t, 1H, NH). ¹³C{¹H} NMR (100.61 MHz, DMSO-*d*₆): δ 50.83 (CH₂), 127.98 (*p*-C_{Ar}-CH₂), 128.51 (*m*-C_{Ph}-P), ³*J*_{CP} = 12.7 Hz), 128.78 (*o*-C_{Ar}-CH₂), 128.12 (*m*-C_{Ar}-CH₂), 129.21 (C₅, ³*J*_{CP} = 12.0 Hz), 130.95 (C₆, ⁴*J*_{CP} = 2.5 Hz), 131.69 (*p*-C_{Ph}-P), 131.78 (C₄, ²*J*_{CP} = 10.6 Hz), 131.94 (*i*-C_{Ph}-P, ¹*J*_{CP} = 85.8 Hz), 132.03 (*o*-C_{Ph}-P, ²*J*_{CP} = 11.0 Hz), 133.38 (C₃, ¹*J*_{CP} = 83.7 Hz), 134.16 (C₂, ²*J*_{CP} = 10.2 Hz), 135.74 (*i*-C_{Ar}-CH₂), 141.77 (C₁, ³*J*_{CP} = 12.4 Hz), 197.53 (C=S). IR (KBr, ν /cm⁻¹): 513, 637 (P=S), 692, 716, 744, 1102, 1407, 1436, 1519 (br, C(S)NH), 2850, 2919, 3028, 3050, 3220. Anal. Calcd for C₂₆H₂₂NPS₂: C, 70.40; H, 5.00; N, 3.16. Found: C, 70.44; H, 5.17; N, 3.11.

Preparation of Pd(L)Cl Complexes 5a,b. A dichloromethane (1.5 mL) solution of PdCl₂(PhCN)₂ (96.9 mg, 0.25 mmol) was added dropwise to a solution of the corresponding ligand **4a,b** (0.25 mmol) in 7 mL of CH₂Cl₂. The reaction mixture was heated over 20 min on a water bath and kept under ambient conditions for 2 days. The resulting precipitate was filtered off, washed with Et₂O (10 mL), and dried in vacuo to give complexes as yellow solids. For **5a** an analytically pure substance was obtained as a DMSO solvate by slow precipitation from DMSO solution using EtOH.

5a. Yield: 72%. Mp: 294–296 °C (dec). ³¹P{¹H} NMR (161.97 MHz, DMSO-*d*₆): δ 58.56 ppm. ¹H NMR (400.13 MHz, DMSO-*d*₆): δ 7.33–7.81 (m, 17H, H_{Ar}), 8.05 (d, 1H, H_{Ar}, ³*J*_{HH} = 8.0 Hz), 12.27 (br s, 1H, NH). ¹³C{¹H} NMR (100.61 MHz, DMSO-*d*₆): δ 122.86 (C₅, ³*J*_{CP} = 13.2 Hz), 125.85 and 125.91 (C_{Ph}-N), 127.89 (C₄, *J*_{CP} = 22.7 Hz), 128.99 (*i*-C_{Ph}-P, ¹*J*_{CP} = 79.7 Hz), 129.47, 129.54, 129.58, 129.66, 129.70 (overlapped signals of *o*-C_{Ph}-P(*d*)+*m*-C_{Ph}-N+C₆), 131.97 (*m*-C_{Ph}-P, ²*J*_{CP} = 11.0 Hz), 133.45 (*p*-

C_{Ph}-P), 137.09 (*i*-C_{Ph}-N), 146.32 (C₃, ¹J_{CP} = 108.8 Hz), 146.95 (C₁, ³J_{CP} = 18.1 Hz), 169.93 (C₂, ²J_{CP} = 26.1 Hz), 199.53 (C=S). IR (KBr, ν/cm⁻¹): 519, 607, 623, 690 (s, P=S-Pd), 707, 720, 749, 1104, 1376, 1438, 1542 (C(N)S-Pd), 1591, 2852, 2921, 3052. Anal. Calcd for C₂₅H₁₉ClNPPdS₂·DMSO: C, 49.93; H, 3.89; N, 2.16. Found: C, 49.74; H, 3.89; N, 2.17.

5b. Yield: 89%. Mp: 287–290 °C (dec). ³¹P{¹H} NMR (161.97 MHz, DMSO-*d*₆): δ 58.58 ppm. ¹H NMR (400.13 MHz, DMSO-*d*₆): δ 5.00 (s, 2H, CH₂), 7.33–7.48, 7.68–7.84 (both m, 7H+11H, H_{Ar}), 7.95 (d, 1H, H_{Ar}), ³J_{HH} = 7.8 Hz), 11.46 (br s, 1H, NH). ¹³C{¹H} NMR (100.61 MHz, DMSO-*d*₆): δ 48.97 (CH₂), 122.81 (C₅, ³J_{CP} = 12.2 Hz), 127.42 (C₆, ⁴J_{CP} = 2.0 Hz), 127.81 (*p*-C_{Ph}-CH₂), 127.93 (*o*-C_{Ph}-CH₂), 128.69 (*m*-C_{Ph}-CH₂), 128.97 (*i*-C_{Ph}-P, ¹J_{CP} = 79.6 Hz), 129.62 (*m*-C_{Ph}-P, ³J_{CP} = 12.7 Hz), 131.94 (*o*-C_{Ph}-P, ²J_{CP} = 11.0 Hz), 133.43 (*p*-C_{Ph}-P), 135.52 (*i*-C_{Ph}-CH₂), 135.75 (C₄, ²J_{CP}=16.0 Hz), 146.29 (C₃, ¹J_{CP} = 108.4 Hz), 146.46 (C₁, ³J_{CP} = 17.7 Hz), 169.28 (C₂, ²J_{CP} = 25.4 Hz), 198.71 (C=S). IR (KBr, ν/cm⁻¹): 516, 525, 607, 624, 694 (s, P=S-Pd), 706, 743, 1100, 1106, 1379, 1435, 1562 (s, C(N)S-Pd), 1578, 2852, 2920, 3100, 3196. Anal. Calcd for C₂₆H₂₁ClNPPdS₂·0.8CH₂Cl₂: C, 49.34; H, 3.49; N, 2.15. Found: C, 49.13; H, 3.30; N, 2.04.

Catalytic Experiments. In a typical experiment a solution of 1 mmol of aryl bromide, 1.5 mmol of PhB(OH)₂, 2 mmol of K₃PO₄, 0.2 mmol of Bu₄NBr, and the mentioned amount of the corresponding palladium complex **5** in 5 mL of DMF was heated at 120 °C over 6 h. After cooling the reaction mixture was immediately analyzed by GC.

Crystal Structure Determination and Data Collection. The details of the X-ray data collection and conventional full-matrix anisotropic-isotropic refinement of **3b**, **5a(A)**, **5a(B)**, and **5b** are listed in Table 5. The multipole refinement of **5b** was carried out

within the Hansen–Coppens formalism using the XD program package with the core and valence electron density derived from wave functions fitted to a relativistic Dirac–Fock solution. Before the refinement the N–H and C–H bond distances were normalized to standard values. The level of multipole expansion was hexadecapole for palladium and chlorine and octupole for phosphorus, sulfur, nitrogen, and carbon atoms. The dipole D₁₀ and the hexadecapoles H₄₀ were refined for all hydrogen atoms for a more accurate description of hydrogen bonds. The refinement was carried out against *F* and converged to *R* = 0.0126, *wR* = 0.0150 and GOF = 1.219 for 8023 merged reflections with *I* > 3σ(*I*). All bonded pairs of atoms satisfy the Hirshfeld rigid-bond criteria (the maximum difference of the mean square displacement amplitudes was 11 × 10⁻⁴ Å²). The residual electron density was not more than 0.5 e Å⁻³. Analysis of the ρ(**r**) function topology was carried out using the WinXPRO program package.

Acknowledgment. The authors are grateful to the Russian Foundation for Basic Research (grants 06-03-32753, 07-03-12196, 08-03-00508) and the Russian Science Support Foundation for financial support and International Science and Technology Center (Project No.G-1361).

Supporting Information Available: Tables giving complete data collection parameters, atomic coordinates, bond distances and angles, and thermal parameters for **3b**, **5a(A)**, **5a(B)**, and **5b**, UV spectra for ligands **4a,b** and corresponding complexes **5a,b** as well as the luminescence spectrum of **5a(B)** at 300 K. This material is available free of charge via the Internet at <http://pubs.acs.org>.

OM8002762